Novel One-Dimensional Organic Conductor Based on Selenium-Containing Bis-Fused Tetrathiafulvalene Derivative, (TSM-TTP)$(I_3)_{5/3}$

Takehiko Mori,* Tadashi Kawamoto, Yohji Misaki,† and Kazuyoshi Tanaka†

Department of Organic and Polymeric Materials, Tokyo Institute of Technology, O-okayama, Tokyo 152

†Department of Molecular Engineering, Graduate School of Engineering, Kyoto University, Yoshida, Kyoto 606-01

(Received January 20, 1998)

A novel selenium-containing bis-fused tetrathiafulvalene donor, TSM-TTP (2,5-bis[4,5-bis(methylseleno)-1,3-dithiol-2-ylidene]-1,3,4,6-tetrathiapentalene) forms a 3 : 5 triiodide salt, (TSM-TTP)$(I_3)_{5/3}$. This salt has uniform one-dimensional columns of the donors, and is isostructural to the corresponding complex of the sulfur analog. This compound shows a high electrical conductivity, 200 S cm^{-1} at room temperature, and undergoes a metal-insulator transition around 20 K. Another insulating (σ_{rt} = 0.03 S cm^{-1}) phase with trimerized columns is also obtained.

Bis-fused tetrathiafulvalene (TTF) derivatives (hereafter abbreviated as TTP (tetrathiapentalene) donors) are excellent organic donors which form highly conducting radical-cation salts with a variety of anions;[1,2] since these donors construct a two-dimensional network for electrical conduction, many of their radical-cation salts are stable metals down to low temperatures. Among them the TTP donor substituted by four methylthio groups, TTM-TTP (2,5-bis[4,5-bis(methylthio)-1,3-dithiol-2-ylidene]-1,3,4,6-tetrathiapentalene) (see Scheme 1), takes an exceptional position, because many of its radical-cation salts are electrical insulators even at room temperature.[1,3] Its iodine salts are, however, good electrical conductors. There are three different iodine salts: (TTM-TTP)I_3, (TTM-TTP)$_2I_3$, and (TTM-TTP)$(I_3)_{5/3}$.[4,5] Although (TTM-TTP)I_3 has 1 : 1 composition, this salt exhibits a high room-temperature conductivity 700 S cm^{-1} and retains its metallic conductivity down to 160 K, below which this salt becomes a Mott insulator. The 1 : 1 composition results in a half-filled energy band, which is responsible for the Mott insulating state at low temperatures.[6] Another salt, (TTM-TTP)$_2I_3$, is an insulator (σ_{rt} = 0.03 S cm^{-1}) with trimerized columns.[4] The third phase (TTM-TTP)$(I_3)_{5/3}$ consists of highly one-dimensional uniform columns of the donors.[5] This salt exhibits a high room-temperature conductivity (200 S cm^{-1}), and undergoes a metal-insulator transition around 20 K.

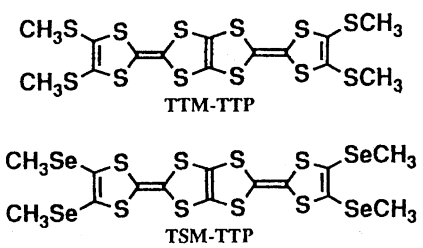

Scheme 1.

The rich variety of chemistry and physics in the iodine salts of TTM-TTP has prompted us to prepare its methylseleno analog, TSM-TTP (see Scheme 1), where the four methylthio groups of TTM-TTP are replaced by methylseleno groups. Electrochemical crystallization has afforded plate-like crystals of (TSM-TTP)$(I_3)_{5/3}$ with characteristic copper luster similarly to (TTM-TTP)$(I_3)_{5/3}$. Here we will described crystal structure and transport properties of (TTM-TTP)$(I_3)_{5/3}$. Together with this major product, a few crystals of another insulating phase have been obtained as a minor product. Although the results are still preliminary, we will also briefly mention the insulating phase.

Results and Discussion

Synthesis. The synthesis of TSM-TTP **1** is outlined in Scheme 2. 4,5-Bis(methylseleno)-1,3-dithiole-2-thione (**2**) was prepared according to Nigrey's procedure.[7] As a protecting group which should be removed after the first phosphite-mediated cross-coupling reaction, 2-cyanoethyl group[8,9] was used instead of acetoxybenzyl group.[1,10,11] On account of the greater stability of the cesium salt than the corresponding sodium salt, this procedure improved the yield of 1,3,4,6-tetrathiapentalen-2-one **4**, typically from 40 to 80%. The availability of the 2-cyanoethyl group was, however, limited by the poor reactivity of **3** in the phosphite-mediated cross-coupling reaction; for example, **3** did not react with unsubstituted 1,3-dithiole-2-thione. On the other hand, deprotection of the acetoxybenzyl group by CsOH brought about decomposition.

Electrochemistry. The solution redox properties of TSM-TTP and TTM-TTP have been studied by cyclic voltammetry. The results are listed in Table 1. These donors show four reversible redox couples up to 4+, which correspond to the oxidation of the four 1,3-dithiole rings. The first redox potential of TSM-TTP is 0.05 V smaller than that of TTM-TTP. This large decrease is, however,

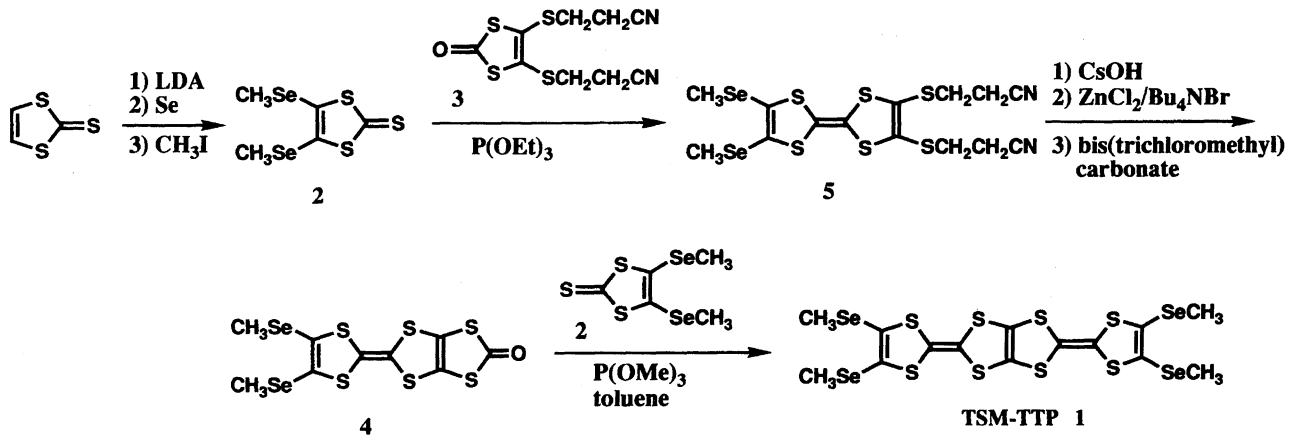

Scheme 2.

Table 1. Half-Wave Redox Potentials (V) vs. Ag/AgCl in (n-Bu)$_4$NPF$_6$/Benzonitrile at a Pt Working Electrode

Compound	E_1	E_2	E_3	E_4	$E_2 - E_1$
TSM-TTP	0.43	0.65	0.97	1.00	0.22
TTM-TTP	0.48	0.67	0.89	1.01	0.19

not surprising in view of the reduced electron withdrawing ability of CH_3Se– in comparison with CH_3S–. In the case of the corresponding TTF analog, TTM-TTF (tetrakis(methylthio)tetrathiafulvalene), the first redox potential of the methylseleno derivative, TSM-TTF (tetrakis(methylseleno)tetrathiafulvalene) is again 0.05 V smaller than that of the methylthio derivative, TTM-TTF.[12]

Electrochemical crystal growth of **1** in the presence of (n-Bu)$_4$NI$_3$ in THF, 1,1,2-trichloroethane, 1,2-dichloroethane, chlorobenzene, or benzonitrile afforded plate-like crystals of (TSM-TTP)$(I_3)_{5/3}$ (3 : 5 phase) with characteristic copper luster. We will designate the 3 : 5 phase as (TSM-TTP)$(I_3)_{5/3}$ instead of (TSM-TTP)$_3(I_3)_5$, because a unit cell contains two TSM-TTP molecules and 5/3 comes from the structure of iodine. When the solvent was THF, a small quantity of black crystals were obtained together with the 3 : 5 phase. Since the insulating phase crystallized in the form of black plates, these crystals were easily distinguished from the 3 : 5 phase by color. Although we attempted the crystal growth under various conditions, the 1 : 1 phase, (TSM-TTP)I_3, was not obtained.

Crystal Structure of (TSM-TTP)$(I_3)_{5/3}$. Crystal data of (TSM-TTP)$(I_3)_{5/3}$, in comparison with (TTM-TTP)$(I_3)_{5/3}$, are listed in Table 2.[5] The lattice constants are almost the same, indicating that these salts are isostructural. All lattice constants of the Se compound are larger than those of the S compound, but the expansion is anisotropic; the increase is large along the b and c axes, namely in the interchain directions.

The atomic numbering scheme of the donor is shown in Fig. 1(a). The atomic coordinates and the equivalent isotropic thermal parameters are listed in Table 3. Similarly to (TTM-TTP)$(I_3)_{5/3}$, the donor is located on a special position of *mmm* symmetry, so that one-quarter of a donor is

Table 2. Crystal Data of (TTM-TTP)$(I_3)_{5/3}$ and (TSM-TTP)$(I_3)_{5/3}$

	(TTM-TTP)$(I_3)_{5/3}$[5]	(TSM-TTP)$(I_3)_{5/3}$	Increase
Formula	$C_{14}H_{12}S_{12}I_5$	$C_{14}H_{12}Se_4S_8I_5$	
F.W.	1199.49	1387.07	
Space group	*Cmmm*	*Cmmm*	
a/Å	6.247(4)	6.259(2)	0.2%
b/Å	18.68(2)	19.14(3)	2.5%
c/Å	12.804(7)	13.068(3)	2.1%
V/Å^3	1494(1)	1565(1)	4.8%
ρ_{calc}/g cm^{-3}	2.666	2.943	
R	0.080	0.077	
Reflections	774	722	

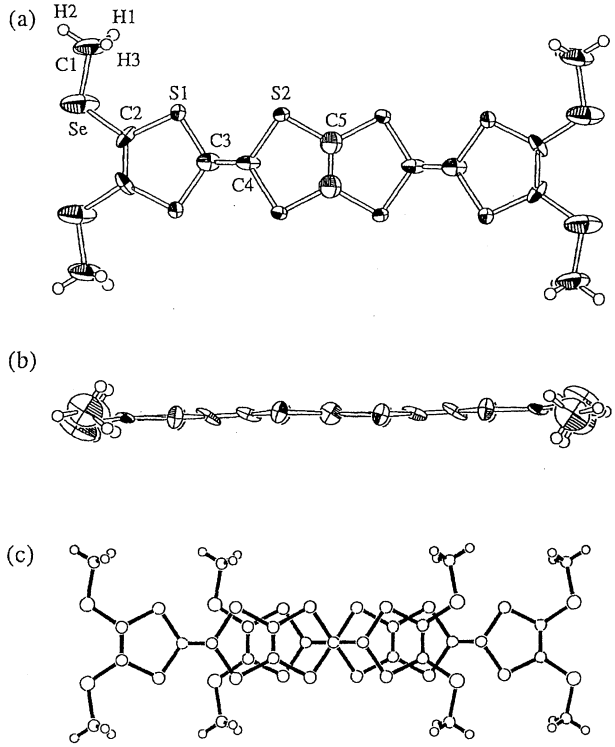

Fig. 1. Structure of (TSM-TTP)$(I_3)_{5/3}$. (a) ORTEP drawing and atomic numbering scheme, (b) side view of the donor molecule, and (c) overlap mode in the stacking direction.

Table 3. Positional Parameters and B_{eq} of (TSM-TTP)$(I_3)_{5/3}$

Atom	x	y	z	B_{eq} [a)]
I(1)	0	0	0	2.64
I(2)	0	0.1528(1)	0	4.47
I(3)	0	0.2512(1)	1/2	4.28
Se	−1/2	0.0868(1)	0.1600(2)	7.3
S(1)	−0.128(1)	0.0766(3)	0.2972(6)	2.7
S(2)	0.287(1)	0.0781(3)	0.4383(5)	2.5
C(1)	−1/2	0.178(1)	0.201(3)	6.7
C(2)	−0.331(5)	0.036(1)	0.234(2)	2.5
C(3)	0	0	0.340(2)	3.2
C(4)	0.159(8)	0	0.395(3)	2.7
C(5)	1/2	0.034(1)	1/2	1.5

a) $B_{eq}=4/3\sum B_{ij}\boldsymbol{a}_i\cdot\boldsymbol{a}_j$.

Table 4. Intramolecular Bond Lengths (Å) and Angles (°) of (TSM-TTP)$(I_3)_{5/3}$

I(1)–I(2)	2.925(2)	I(3)–I(3)	3.130(1)
Se–C(1)	1.82(3)	Se–C(2)	1.72(2)
S(1)–C(2)	1.70(3)	S(1)–C(3)	1.76(1)
S(2)–C(4)	1.79(3)	S(2)–C(5)	1.77(1)
C(2)–C(2)	1.40(5)	C(3)–C(4)	1.23(5)
C(5)–C(5)	1.31(4)		
C(1)–Se–C(2)	112(1)	Se–C(2)–S(1)	119(2)
Se–C(2)–C(2)	124.0(9)	S(1)–C(2)–C(2)	116.8(8)
C(2)–S(1)–C(3)	96.7(9)	S(1)–C(3)–S(1)	112.9(9)
S(1)–C(3)–C(4)	123.6(5)	S(2)–C(4)–C(3)	123(1)
S(2)–C(4)–S(2)	113(3)	C(4)–S(2)–C(5)	95(1)
S(2)–C(5)–C(5)	118.3(6)		

crystallographically independent. As shown in Fig. 2(a), the donors form a uniform stack along the a axis. On account of the *mmm* symmetry, the donor molecules are disordered; there coexist molecules with two kinds of slopes: downward (Fig. 2(a)) and upward (Fig. 2(b)).

The donor molecule is essentially planar; the deviations from the least-squares plane are, including the methyl carbons of the methylseleno parts, less than 0.26 Å (Fig. 1(b)). The intramolecular bond lengths are listed in Table 4. Owing to the disorder, the bond lengths are not accurate enough to estimate the amount of the positive charge located on a donor molecule.

The interplanar distance of the neighboring donors in a stack is 3.44 Å (cf. 3.39 Å for (TTM-TTP)$(I_3)_{5/3}$).[5] The overlap mode is depicted in Fig. 1(c); the donors are displaced by 5.2 Å along the molecular long axis (cf. 5.3 Å for (TTM-TTP)$(I_3)_{5/3}$).[5]

There are two kinds of anions (Fig. 2(c) and (d)). One is discrete I_3^-, which occupy I(1) and I(2) sites, located on the origin with *mmm* symmetry, and extending along the b axis. The I(1)–I(2) distance, 2.925(2) Å, is typical of I_3^-. Since the I(2)–I(2) distance between the neighboring I_3^- is as long as 4.86 Å, these anions are regarded as discrete I_3^-.

The other anion site is I(3). The adjacent I(3)–I(3) distance is as short as $a/2=3.13$ Å, the I(3) atoms thus form an infinite chain along the a axis. It is well known that iodine anions frequently form infinite chains, where the actual unit which constitutes the chain is I^-, I_3^-, or I_5^-.[13] In the average structure analysis such as the present analysis, however,

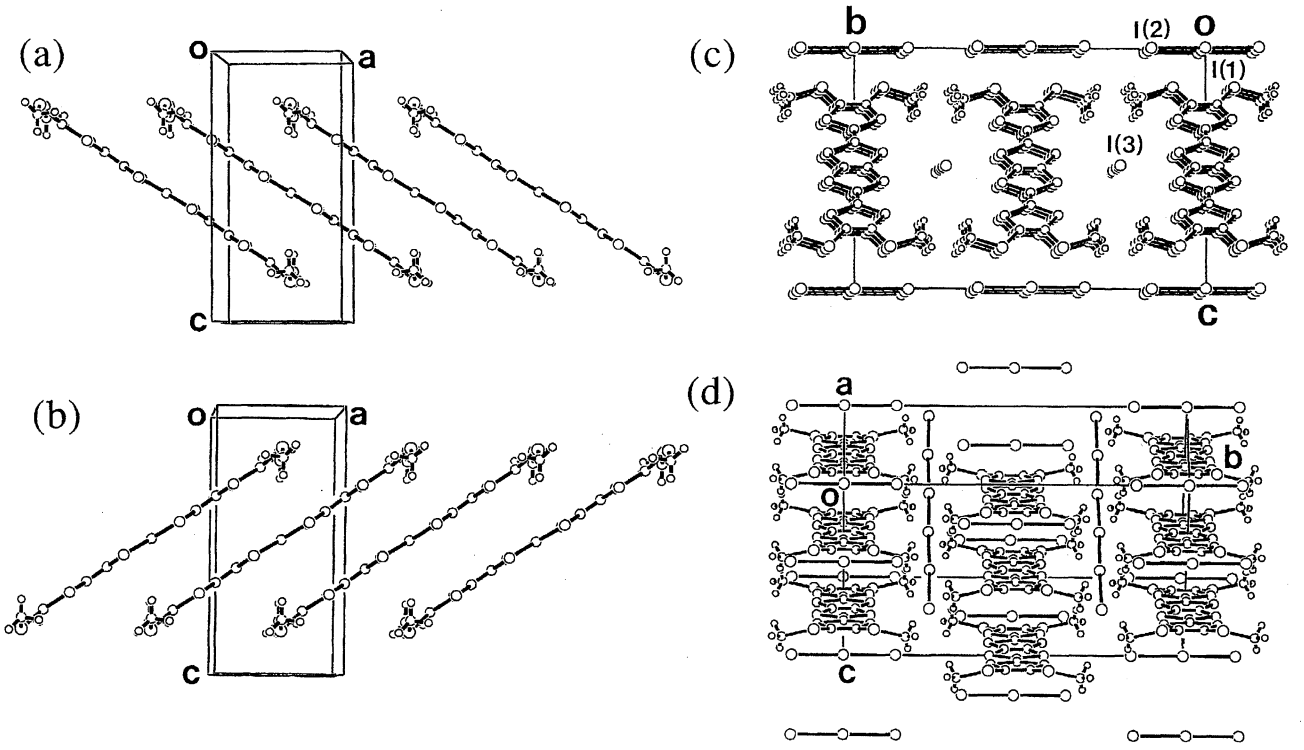

Fig. 2. Crystal structure of (TSM-TTP)$(I_3)_{5/3}$. (a) (b) Projection along the b axis, two possibilities of the disordered donor molecules, (c) projection along the a axis, and (d) view from the donor's molecular long axis.

an infinite chain with regular intervals is observed instead. The average iodine spacing, 3.13 Å, is typical of an infinite I_3^- or I_5^- chain. In the present case the oscillation photographs along the *a* axis showed a few spots at $a^*/3$. The repeating unit $3a = 18.8$ Å is too long for a repeating unit of an I_5^- chain (typically 15.5 Å), and also contradicts the restriction that this unit should contain $2\times3=6$ iodine atoms. By contrast, this superstructure is reasonably interpreted by assuming the periodicity of $(3/2)a = 9.39$ Å, which is the typical length of the repeating unit of the infinite I_3^- chain. From the structure analysis, we can conclude that the anion part is composed of the discrete I_3^- and the infinite chain of I_3^-, both without any observable deficiency. The accurate composition is $(TSM\text{-}TTP)(I_3)(I_3)_{2/3}$, or $(TSM\text{-}TTP)(I_3)_{5/3}$, and the donor maintains a large positive charge of +5/3.

Because the donor chains are separated from each other by the two kinds of iodine units: along the *c* axis by the discrete I_3^- and along the *b* axis by the infinite I_3^- chain, the electronic structure is highly one-dimensional. The transfer integrals calculated from the overlap of HOMO are $t_a = 0.165$ eV (along the stack), $t_c = 0.013$ eV, and $t_b = 3\times10^{-4}$ eV (interchain) (cf. $t_a = 0.157$ eV, $t_c = 0.03$ eV, and $t_b = 4\times10^{-4}$ eV for $(TTM\text{-}TTP)(I_3)_{5/3}$.[5] In comparison with the sulfur analog, the intrachain transfer integral t_a increased slightly, but the interchain interactions t_c and t_b decreased. Then the selenium compound exhibits higher one-dimentionality than the sulfur compound. This is reasonable because the expansion of the lattice occurs principally in the interchain (b and c) directions (see Table 1).

Tight-binding energy band structure and Fermi surface, calculated on the basis of the above transfer integrals, are depicted in Fig. 3. The energy band is basically one-dimensional along the *a* axis, and the Fermi surface is more planar than that of the sulfur compound. The calculated bandwidth is 0.71 eV. On account of the high oxidation state of the donors, the Fermi surface is located very close to the XB boundary, so this energy band is one sixth filled. However, when we take the three-fold superstructure into account, one-sixth filled corresponds to half-filled. The effectively half-filled band exerts a serious influence to the magnetic properties, as will be discussed in a separate paper.[14]

Transport Properties. Electrical resistivity of $(TSM\text{-}TTP)(I_3)_{5/3}$ is shown in Fig. 4(a). The room-temperature conductivity is 200 S cm^{-1}; this value is exactly the same as that of $(TTM\text{-}TTP)(I_3)_{5/3}$. Although the resistivity of $(TTM\text{-}TTP)(I_3)_{5/3}$ shows metallic decrease down to about 250 K, that of $(TSM\text{-}TTP)(I_3)_{5/3}$ is almost constant and starts to increase gradually below 200 K. However the steep rise occurs below 20 K; this temperature is about the same as $(TTM\text{-}TTP)(I_3)_{5/3}$.

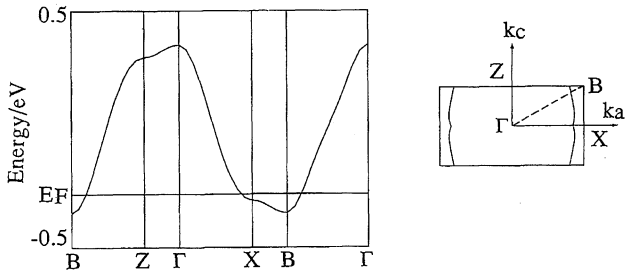

Fig. 3. Energy band structure and Fermi surface of $(TSM\text{-}TTP)(I_3)_{5/3}$.

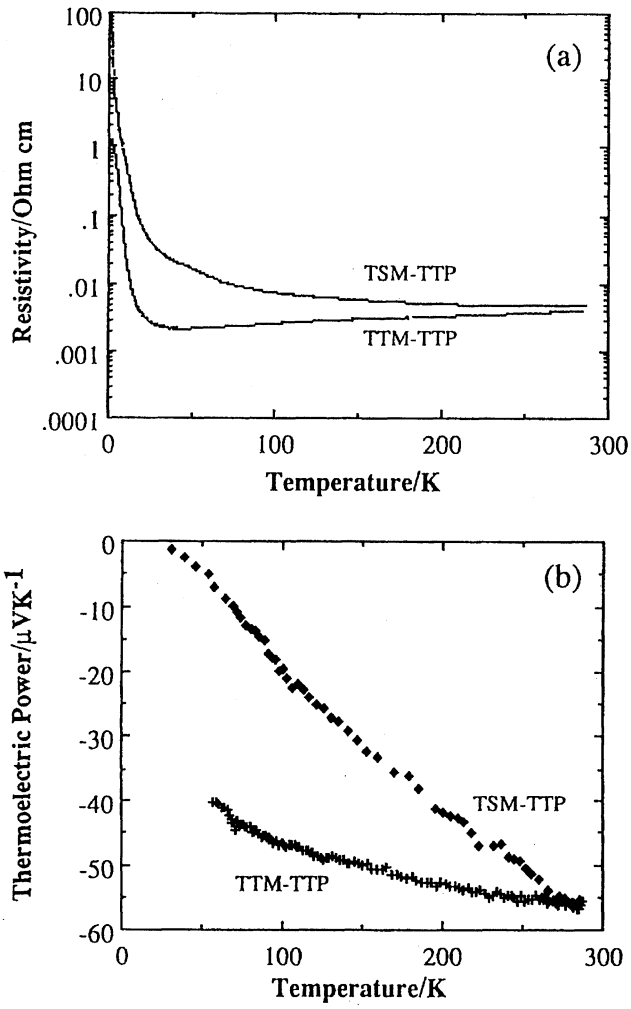

Fig. 4. (a) Electrical resistivity and (b) thermoelectric power of $(TTM\text{-}TTP)(I_3)_{5/3}$ and $(TSM\text{-}TTP)(I_3)_{5/3}$.

As shown in Fig. 4(b), the thermoelectric power is negative. This is associated with the large charge transfer that exceeds half-filled; the HOMO band is less than half-filled, leading to electron-like conduction and negative thermoelectric power. The room-temperature value, -56 μV K^{-1} is almost the same for TTM-TTP and for TSM-TTP, from which, by assuming the one-dimensional tight-binding band, we can estimate the bandwidth to be 0.38 eV. Although not shown in Fig. 4(b), in the insulating region (< 20 K), the thermoelectric power gradually diverges.

Insulating Phase. Together with the above mentioned $(TSM\text{-}TTP)(I_3)_{5/3}$, a few black crystals are obtained as a minor product. Although the crystal structure analysis is preliminary, we will describe the outline of the crystal structure.

Crystal data of $(TSM\text{-}TTP)_3(I_3)_2$: $C_{42}H_{36}S_{24}Se_{12}I_6$, F.W. 3019.13, triclinic, space group $P\bar{1}$, $a = 13.69(4)$, $b = 14.05(2)$,

$c = 12.46(1)$ Å, $\alpha = 109.32(6)$, $\beta = 116.2(1)$, $\gamma = 77.2(1)^\circ$, $Z = 1$, $\rho_c = 2.48$ g cm^{-3}, and $V = 2022(6)$ Å^3. The structure is shown in Fig. 5. One and half units of the donor molecules are crystallographically independent; molecule A is located on a general position and molecule B on an inversion center. The donors make trimerized columns along the c axis, where a trimer is made up of an ABA unit. In the intertrimer overlap (c2), the molecules are displaced not only along the molecular long axis, but also along the molecular short axis.

The iodine atoms form discrete I_3^-, which are placed between the donor chains so as to separate the donor chains. The direction of the I_3^- unit is approximately parallel to the stacking axis (c axis). The c axis (12.46(1) Å) is a little longer than I_3^- (9.4 Å), so that four iodine atoms are able to be incorporated within the repeating unit. This iodine disorder is responsible for the failure of the structure analysis.

If we do not take the iodine disorder into account, one trimer of the donors and two I_3^- units are incorporated in a unit cell, thereby composition is $(TSM\text{-}TTP)_3(I_3)_2$. From the energy dispersion spectroscopy, the S : I ratio is 8 : 5.12, suggesting that the donor : I_3^- ratio is 1 : 0.64. Because this ratio is close to 3 : 2, we consider that the approximate composition is $(TSM\text{-}TTP)_3(I_3)_2$.

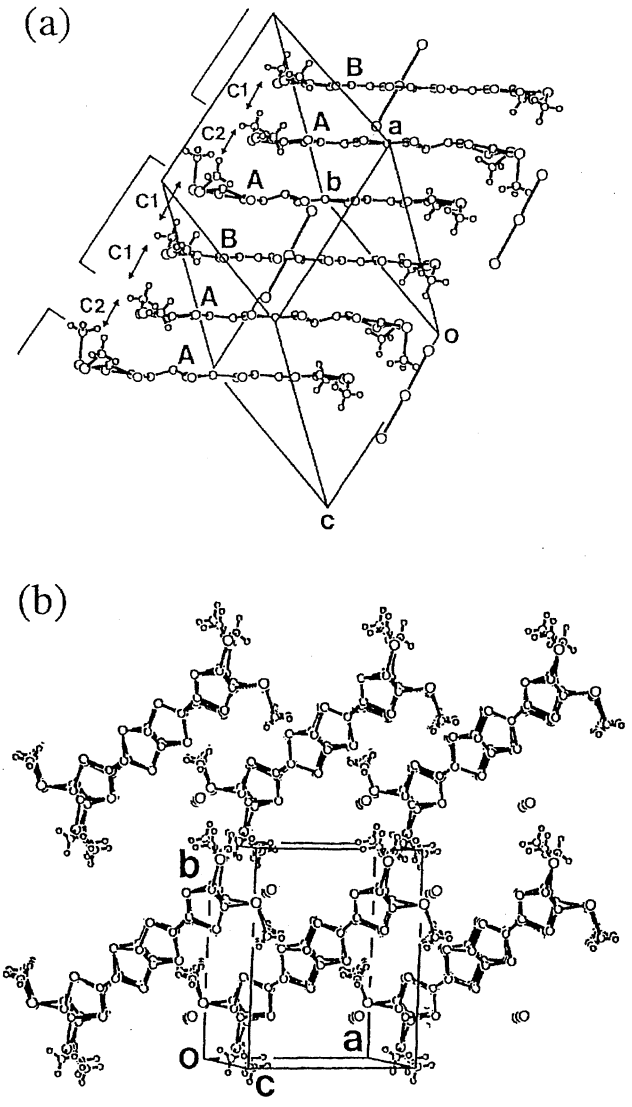

Fig. 5. Crystal structure of $(TSM\text{-}TTP)_3(I_3)_2$. (a) Structure of the column, and (b) projection along the stacking direction.

The 3 : 2 composition results in a two-thirds filled HOMO band, giving rise to a band insulator. The room-temperature conductivity is 0.03 S cm^{-1} and the activation energy is 0.2 eV. These values are close to those of $(TTM\text{-}TTP)_2I_3$ (0.03 S cm^{-1} and 0.3 eV),[4] which has also trimerized columns, although the crystal structure is different.

In conclusion, we have prepared TSM-TTP, a methylseleno analog of TTM-TTP. Electrocrystallization of TSM-TTP has afforded two phases: $(TSM\text{-}TTP)(I_3)_{5/3}$ as a major product and an insulator phase as a minor product. The 1 : 1 salt $(TSM\text{-}TTP)I_3$ has not been obtained. $(TSM\text{-}TTP)(I_3)_{5/3}$ is isostructural to $(TTM\text{-}TTP)(I_3)_{5/3}$. $(TSM\text{-}TTP)(I_3)_{5/3}$ has one-dimensional columns of the donors, and the anion is composed of discrete I_3^- and "infinite" chain of I_3^-. This salt undergoes a metal-insulator transition at 20 K. Measurements exploring the origin of this transition are now in progress.[14]

Experimental

Synthesis. 4,5-Bis(methylseleno)-1,3-dithiole-2-thione (**2**)[7] (0.72 g, 2.5 mmol) and 4,5-bis(2-cyanoethylthio)-1,3-dithiole-2-one (**3**)[8] (0.8 g, 2.5 mmol) were heated in triethyl phosphite (9 ml) at 110 °C under argon atmosphere for 2 h. After the triethyl phosphite was evaporated in vacuo, the residue was chromatographed on silica gel with CS_2/CH_2Cl_2 as the eluent to afford an orange solid, 2,3-bis-(2-cyanoethylthio)-6,7-bis(methylseleno)tetrathiafulvalene (**5**), 0.59 g (42 %), mp 112 °C; ^{1}H NMR (CD_3Cl) $\delta = 2.36$ (6H), 2.74 (4H), 3.06 (4H); IR (KBr) 2909 (m), 2250 (m), 1420 (s), 1266 (m), 888 (m), 770 (m) cm^{-1}; MS m/z 562 (M^+).

The tetrathiafulvalene (**5**) (0.56 g 0.99 mmol) and $CsOH\cdot H_2O$ (1.77 g, 12 mmol) were reacted in acetone (3 ml) and methanol (3 ml) under argon atmosphere for 1 h. Zinc chloride (0.12 g, 0.88 mmol) dissolved in 2.5 ml methanol and tetrabutylammonium bromide (0.34 g, 1.0 mmol) in 2.5 ml methanol were successively added. The formed precipitates were collected by filtration, and washed by methanol, and dried in vacuo. The residue was suspended in THF (9 ml), cooled to −70 °C. Bis(trichloromethyl) carbonate (triphosgen, 0.2 g, 0.42 mmol) in THF was dropwise added to the suspension, and the reaction mixture was allowed to warm up to room temperature. The solvent was removed by a rotary evaporator, methanol was added, and the residue was collected by filtration and washed by water and methanol, and dried in vacuo to yield 0.38 g (80 %) brown solid, 5-[4,5-bis(methylseleno)-1,3-dithiol-2-ylidene]-1,3,4,6-tetrathiapentalen-2-one (**4**), mp 166—173 °C; ^{1}H NMR (CS_2–CD_3Cl) $\delta = 2.32$ (6H); IR (KBr) 1668 (s) cm^{-1} (C=O); MS m/z 480 (M^+).

The tetrathiapentalenone **4** (0.38 g, 0.79 mmol) and 4,5-bis-(methylseleno)-1,3-dithiole-2-thione (**2**) (0.51 g, 1.59 mmol) were reacted in 13 ml trimethyl phosphite and 13 ml toluene at 110 °C under argon atmosphere for 2 h. The reaction mixture was cooled, and the resulting precipitate was filtered off, washed with hexane and methanol, and dried in vacuo. Chromatography (silica gel, CS_2) afforded orange crystals **1**, 95 mg (16 %), mp 186—192 °C; ^{1}H NMR (CS_2–CD_3Cl) $\delta = 2.33$ (12H); IR (KBr) 2920 (w), 1505

(w), 1412 (w), 1384 (w) cm^{-1}.

X-Ray Crystallography. Intensity data were collected by the Rigaku Raxis II area detector with graphite monochromated Mo $K\alpha$ radiation ($\lambda = 0.71070$ Å) at room temperature. As for (TSM-TTP)$(I_3)_{5/3}$, because the structure was expected to be isostructural to (TTM-TTP)$(I_3)_{5/3}$, the atomic coordinates were taken from the results of (TTM-TTP)$(I_3)_{5/3}$.[5] All non-hydrogen atoms were refined anisotropically. Hydrogen atoms were included but not refined. Neutral atomic scattering factors were taken from "International Tables."[15] The final cycle of full-matrix least-squares refinement ($w = 1/\sigma(F_o)^2$) converged to $R = 0.077$ and $R_w = 0.084$ based on 722 observed reflections ($2\theta < 60°$ and $I > 5\sigma(I)$).

T. Kawamoto is grateful to the JSPS Research Fellowship for Young Scientists for financial support.

References

1) Y. Misaki, H. Nishikawa, K. Kawakami, S. Koyanagi, T. Yamabe, and M. Shiro, *Chem. Lett.*, **1992**, 2321.

2) T. Mori, T. Kawamoto, Y. Misaki, K. Kawakami, H. Fujiwara, T. Yamabe, H. Mori, and S. Tanaka, *Mol. Cryst. Liq. Cryst.*, **284**, 271 (1996).

3) Y. Misaki, H. Nishikawa, T. Yamabe, T. Mori, H. Mori, and S. Tanaka, *Synth. Metals*, **70**, 1153 (1995).

4) T. Mori, H. Inokuchi, Y. Misaki, T. Yamabe, H. Mori, and S. Tanaka, *Bull. Chem. Soc. Jpn.*, **67**, 661 (1994).

5) T. Mori, Y. Misaki, and T. Yamabe, *Bull. Chem. Soc. Jpn.*, **70**, 1809 (1997).

6) T. Mori, T. Kawamoto, J. Yamaura, T. Enoki, Y. Misaki, T. Yamabe, H. Mori, and S. Tanaka, *Phys. Rev. Lett.*, **79**, 1702 (1997).

7) P. J. Nigrey, *Synth. Met.*, **27**, B365 (1988).

8) N. Svenstrup, K. M. Rasmussen, T. K. Hansen, and J. Becher, *Synthesis*, **1994**, 809.

9) L. Binet, J. M. Fabre, C. Montginoul, K. B. Simonsen, and J. Becher, *J. Chem. Soc., Perkin Trans. 1*, **1996**, 783.

10) Y. Misaki, K. Kawakami, H. Fujiwara, T. Miura, T. Kochi, M. Taniguchi, T. Yamabe, T. Mori, H. Mori, and S. Tanaka, *Mol. Cryst. Liq. Cryst.*, **296**, 77 (1997).

11) C. Gemmell, J. D. Kilburn, H. Ueck, and A. E. Underhill, *Tetrahderon Lett.*, **33**, 3923 (1992).

12) N. Iwasawa, G. Saito, K. Imaeda, T. Mori, and H. Inokuchi, *Chem. Lett.*, **1987**, 2399.

13) P. Coppens, "Extended Linear Chain Compounds I," ed by J. S. Miller, Plenum, New York (1982), p. 333.

14) T. Kawamoto, T. Mori, Y. Misaki, K. Tanaka, H. Mori, and S. Tanaka, *Physica C*, **299**, 36 (1998).

15) D. T. Cromer and J. T. Weber, "International Tables for X-Ray Crystallography," Kluwer Academic Publishers, Boston (1992), Vol. C.

16) G. M. Sheldrick, "Crystallographic Computing 3," Oxford University Press, Oxford II (1985), pp. 175—189.